Prediction of rib fractures to elderly female occupants by means of a combination of anterior-posterior and lateral deformation of the rib cage in a near-side crash

Takayuki Kawabuchi, Hisaki Sugaya, Yukou Takahashi
Amanda Agnew, Yun-Seok Kang, John Bolte IV

Abstract Seat belt pretensioners (SBPT) cause deflection of the rib cage anteroposteriorly even in a side crash. Since the maximum value of anterior-posterior (A/P) deflection is generally smaller than that of lateral deflection in a side crash, probability of thoracic injury has been assessed by lateral deflection. However, the contribution of A/P deflection may be relatively large in low-speed crashes where lateral deflection tends to be smaller. The objective of this study is to investigate the relative contribution of A/P deflection due to SBPT activation to the predicted number of fractured ribs (NFR) with human body model (HBM) simulations. The HBM simulations showed that predicted NFR increased from 1 to 4 by the activation of SBPT at a delta-V of 16 km/h, which would raise the fatality rate of the elderly population. The injury metrics named Bent Rib Index (BRI) and Thoracic Area Index (TAI) using the combination of A/P and lateral deflection showed a better correlation with predicted NFR than that using lateral deflection alone (LCmax). The coefficient of determination were 0.87, 0.88 and 0.76 for BRI, TAI and LCmax, respectively.

Keywords low-speed side crash, seat belt pretensioner, thoracic injury, number of fractured ribs, elderly female occupants

I. INTRODUCTION

According to the results from an accident data analysis [1], approximately 6.7 million passengers were involved in crashes in the United States in 2018. Among all accident types, frontal and side crash accounts for 64% and 21%, respectively. Among all combinations of non-rollover crash types and age ranges of drivers sustaining Maximum Abbreviated Injury Scale (MAIS) 4+ injuries, the percentage of drivers aged 65 or older involved in a near-side crash was the largest, which was nearly a double of that of the second most frequent combination of drivers aged between 45 and 64 involved in a near-side crash [2]. These results suggest that elderly drivers in a near-side crash tend to sustain more serious injuries compared to other combinations of crash types and occupant ages. Reference [3] predicted that the elderly population will expand to 83.7 million by the year 2050 from 43.1 million in 2012 in the United States. Therefore, it is critical to improve protection performance for elderly occupants in near-side crashes.

The percentage of injuries to the thorax is the largest of all body regions for elderly occupants in near-side crashes. In particular, elderly female occupants aged 71 or older showed larger percentage than that of male [4]. In addition, the fatality rate of elderly trauma patients with rib fractures was 20.1 %, which was larger than 7.6 % for those without rib fractures [5]. For these reasons, it is crucial for elderly female occupant protection to reduce the probability of rib fractures.

Previous studies have identified the relationship between rib fractures and thoracic compression [6-7] by analyzing force-deflection data of the struck-side half-thorax and acceleration data of the thoracic spine in a series of cadaveric lateral drop tests from heights of 1 to 3 m onto both unpadded and padded force plates. They found that a maximum compression of 35% to the struck-side thorax resulted in Abbreviated Injury Scale (AIS) 3+ injuries, and that maximum compression better predicted the probability of injuries than maximum chest acceleration. Researchers [8] analyzed the results of 17 Post Mortem Human Subjects (PMHS) tests using the Heidelberg-type lateral sled setup and found that a maximum thoracic compression of 31%, including arm deformation, corresponded to a 25% chance of sustaining AIS 4+ thoracic injuries. A separate study [9] analyzed the results of the 34 PMHS tests using a Heidelberg-type lateral sled setup and found maximum thoracic deflection (dmaxn)

T. Kawabuchi is an Assistant Chief Engineer (e-mail: Takayuki_Kawabuchi@jp.honda, tel: +81 80 4906 9631), H. Sugaya is an Assistant Chief Engineer and Y. Takahashi is a Chief Engineer at Honda R&D Co., Ltd., Tochigi, Japan. A. Agnew, PhD is an Associate Professor, Y. Kang, PhD is an Assistant Professor and J. Bolte IV, PhD is a Professor at the Injury Biomechanics Research Center, The Ohio State University, Columbus, OH, US

better correlated with AIS 4+ rib fractures than the Thoracic Trauma Index defined by [10]. Due to the findings of these past studies, maximum lateral deflection has been widely used as an injury prediction criterion (IPC) for a side impact Anthropomorphic Test Device (ATD), such as the World SID ATD [11].

On the other hand, the thorax of the occupants may undergo not only lateral deflection but also anterior-posterior (A/P) deflection due to an activation of the seat belt pretensioner (SBPT). Recently researchers conducted PMHS near-side sled tests using mass production SBPT and a side airbag [12]. The test results showed that the A/P deflection caused by the SBPT activation and the lateral deflection were 14.4 and 9.4 mm, respectively, when the rib fracture occurred on the anterior region of the thorax. It suggested that the rib fracture may occur even by the small lateral deflection due to the contribution of A/P deflection in a side crash. As it is expected that the low-speed impact with the small lateral deflection would spread by an improvement and a dissemination of the automatic emergency braking system, it may increase in importance to consider the relative contribution of A/P deflection in order to reduce the probability of the thoracic injury. To date, there has not been a research conducted which focused on the effects of SBPT on rib fractures in a side crash. In addition, low-speed PMHS side sled tests have not been conducted.

The objective of this study is to investigate that the relative contribution of A/P deflection to the predicted number of fractured ribs (NFR) is high in a low-speed crash by means of finite element (FE) simulations. The study also investigated the injury metrics combining A/P deflection with lateral deflection correlated with the predicted NFR in a side crash.

II. METHODS

The accident data analysis

The accident data analysis was conducted to investigate the relationship of the SBPT activation and NFR to elderly female occupants in near-side crash. The NFR, statuses of the SBPT activation and generative delta-V were aggregated from the public portal of National Automotive Sampling System – the Crashworthiness Data System (NASS-CDS) [13] and Crash Injury Research and Engineering Network (CIREN) [14] databases for the years 2004-2015. The inclusion criteria were female occupants using a seat belt aged 65 or older with rib fractures involved in a direction of force (DOF) between 60 to 120 degrees and 240 to 300 degrees, for right-side and left-side occupants, respectively, which were corresponding to a near-side impact. The NFR were non-weighted values and aggregated from a description of specific injury aspects included in NASS-CDS and CIREN databases. As a result, the number of samples were both 13 with and without the SBPT activation.

The data were divided into 2 generative delta-V groups: less than 28 km/h (< 28km/h) and 28 km/h or more (>= 28 km/h). The boundary delta-V of 28 km/h was the mode of the frequency of the delta-V with elderly female occupants sustaining AIS 3 [15]. Therefore, an occupant in the >= 28 km/h group was assumed to sustain more severe injury than that in < 28 km/h group. For each delta-V group, mean values of the NFR were t-tested between the two groups with and without SBPT activation by assuming homogeneity of variance.

FE simulations with Human Body Model

The influence of the SBPT activation on a predicted NFR in a near-side crash was investigated by FE simulations with a human body model (HBM). The HBM used in this study was an in-house model on LS-DYNA (version R7.1 LSTC, Livermore, CA, USA) which was developed by [16]. The HBM was geometrically scaled and the density of the internal organs were adjusted to represent female elderly population. The stature and weight of HBM were 151 cm and 47 kg, respectively, which represented 5th percentile female in the United States based on [17]. Figure 1 shows the model configuration representing the environment in a mass-production small-size sedan, including a 3-point seat belt with pretensioner, a side airbag, a seat and a door panel. A side airbag extended out from the seat in order to ensure the inflation and a side curtain airbag was represented by a block element with a characteristic of a urethane foam having a 30 times foaming ratio.

The near-side crash FE simulation was validated in a previous study [18] against a PMHS sled test (subject #2) in a near-side crash described in [12]. The PMHS sled test simulated a driver in a small-size sedan undergoing a near-side impact at a delta-V of 30 km/h. The SBPT was represented by applying the time history of the seatbelt tensile force measured between a D-ring and a retractor in the PMHS test. The SBPT generates peak force within approximately 3 ms after the activation.

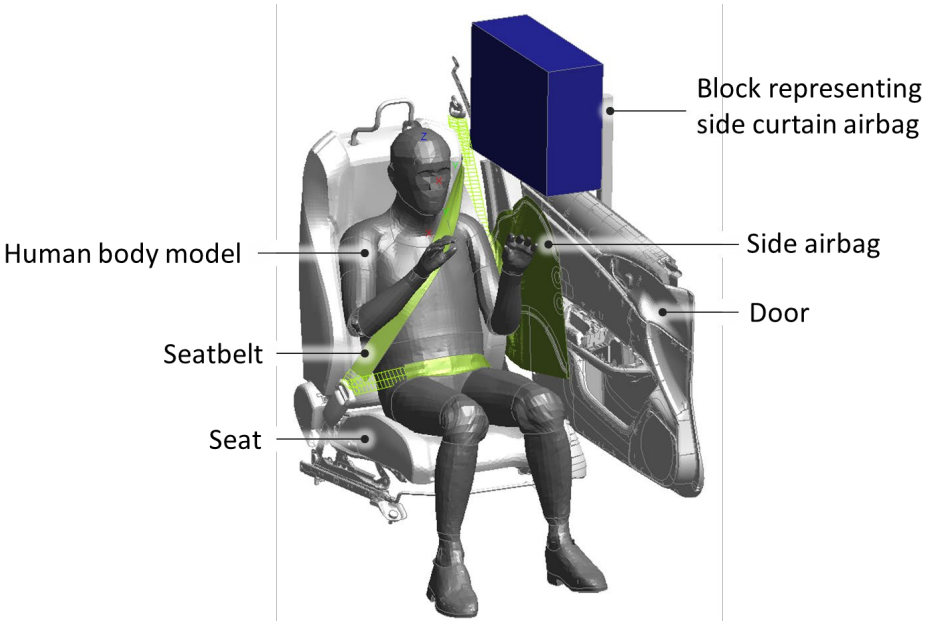

Fig. 1. The configuration of HBM simulation

The measurement points of both lateral and A/P deflections are shown in Figure 2. Lateral deflection was measured on the 1st through 10th ribs at the mid-axillary line on the lateral surface of each rib. The measurement points for A/P deflection were defined by the intersection between the center line of the sternum surface and the horizontal plane passing through the anterior tips of the 1st to 7th ribs.

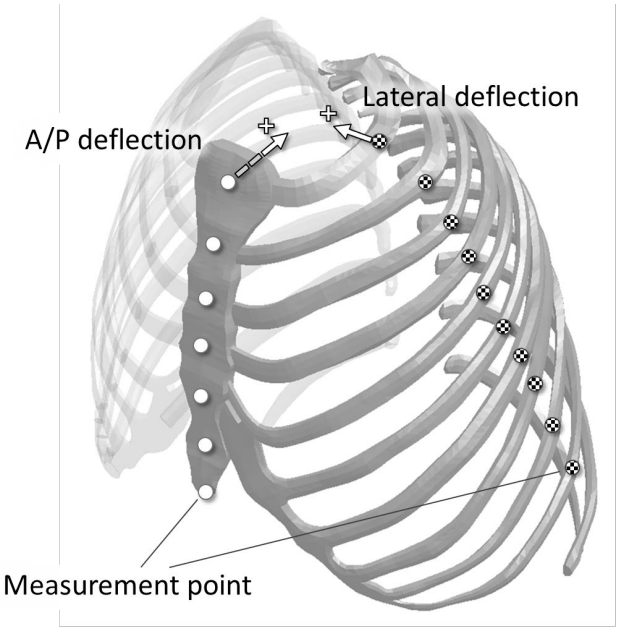

Fig. 2. Deflection measurement points and the positive direction of deflection

The acceleration pulses were created by a FE simulation in which the Moving Deformable Barrier (MDB) defined in the Federal Motor Vehicle Safety Standard 214 was made to collide with a mass-production small-size sedan at three delta-V levels based on the accident data analysis in the previous study [15], which were 16, 24 and 30 km/h, representing the delta-V in crashes with elderly female occupants sustaining AIS 2, AIS 3 and AIS 4, respectively.

A door panel were divided into quadrant regions and produced lateral movements independently, which were in accordance with the time-historical motion extracted from the FE simulations at each delta-V.

In the HBM simulations, rib fractures were represented by the maximum principal strain (MPS) of the elements

for a rib cortical bone exceeding 0.022, which was the fracture threshold for an elderly occupant defined according to the average value of ultimate failure strain gained from the cortical bone coupon tests [19].

Investigation of injury metrics for the predicted NFR

The relationship between a predicted NFR and a rib deflection was investigated with these FE simulations by means of A/P and lateral deflection measured at the points shown in Figure 2. Three injury metrics were created in this study and their prediction capabilities were assessed by the coefficient of determination (R^2). The first one used the maximum value of the lateral normalized deflection among ribs 1-10, which was defined as LCmax. The concept is based on current IPCs such as Dmax used in legislation or assessment test programs. The formulation of LCmax is given by equation (1)

$$\mathrm{LCmax} = \max[LC_i] \tag{1}$$

Where, LC is lateral deflection normalized by the chest width, 293 mm. The suffix i represents the number of each rib.

The second injury metric used a combination of lateral and A/P normalized deflection. A conceptual image of the injury metric is shown in Figure 3. This injury metric, defined as Bent Rib Index (BRI), was based on the assumption that the combination of lateral and A/P deflections would increase the curvature of rib and result in increasing strain on the center point of the bent rib. The formulation of BRI is given by equation (2).

$$\mathrm{BRI} = \max[\, LC_i + AP_i \,] \tag{2}$$

Where, AP_i and LC_i represent the A/P and lateral normalized deflections. AP_i was A/P deflection normalized by a chest depth of 207 mm. LC_i was the same as that used in LCmax. The suffix i takes the number from 1 to 10, rib number. As shown in Figure 2, the maximum number for the measurement points on the sternum is seven.

The third injury metric used a product of width and depth of the thorax. This injury metric was based on the assumption that the concurrent compression of a rib cage in the A/P and lateral direction would increase a probability of rib fracture as suggested in past research [12]. The product of compressed width and depth of the thorax was assumed to be correlated with the severity of rib fracture. Figure 4 shows the conceptual image of the injury metric. The severity of rib fracture is assessed by the conceptual area which is the difference of the product of minimum width and depth from the initial area. Thus, the smaller the rib cage becomes by the compression, the larger the injury metric and the likelihood of fracture become. The injury metric was defined as Thoracic Area Index (TAI) and its formulation is given by equation (3.1) and (3.2).

$$TAI = \max[1 - A_i] \tag{3.1}$$

$$A_i = \min(1 - \mathrm{AP_i}) \times \min(1 - \mathrm{LC_i}) \tag{3.2}$$

Where, AP_i and LC_i are the same as those used in LCmax. The suffix i is the index for each rib as mentioned in the definition of BRI.

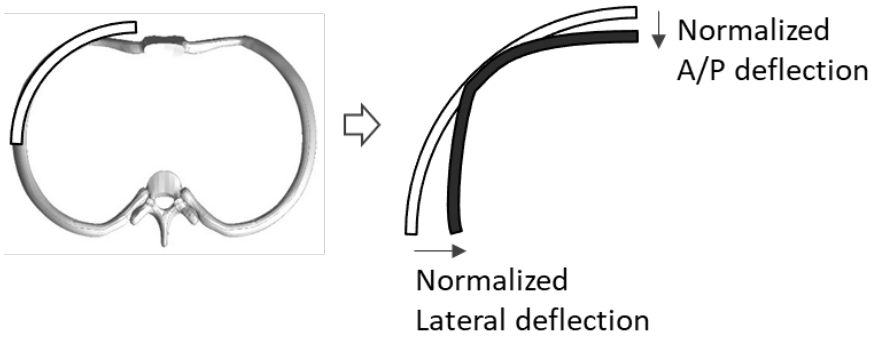

Fig. 3. A conceptual image of BRI

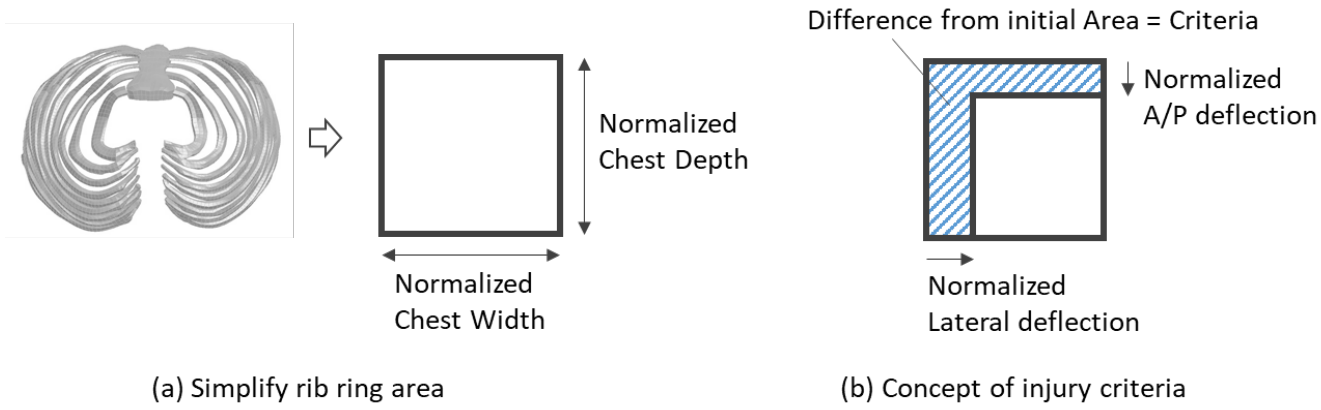

Fig. 4. A conceptual image of TAI

III. RESULTS

The accident data analysis

Table I shows the number of data, mean NFR and p-values for each delta-V group. Both delta-V groups showed that mean NFR with an SBPT activation was larger than that without an SBPT activation, whereas they showed no significant differences. The difference between mean NFR with and without the SBPT of <28 km/h group was larger than that of >=28 km/h group.

TABLE I
SUMMARY OF THE ACCIDENT ANALYSIS

	Number of Data		Mean NFR		
Delta-V	With SBPT	Without SBPT	With SBPT	Without SBPT	p-value
< 28 km/h	10	3	5.9	4.0	0.322
>= 28 km/h	3	10	8.0	7.1	0.896

FE simulations with Human Body Model

Table II shows the results of the predicted NFR by HBM simulations with and without the SBPT in each delta-V. The predicted NFR with SBPT was larger than that without the SBPT at 16 and 24 km/h however no difference of those was seen at 30 km/h.

TABLE II
SUMMARY OF THE PREDICTED NFR BY HBM SIMULATIONS

	Predicted NFR	
Delta-V	With SBPT	Without SBPT
16 km/h	4	1
24 km/h	6	5
30 km/h	8	8

Figure 5 illustrates the MPS with and without the SBPT of each rib. The dashed line indicates the fracture threshold, 0.022. The MPS with the SBPT was larger than that without the SBPT, except for 4th and 5th ribs at 30 km/h. The maximum differences of the MPS with and without the SBPT were 0.030, 0.029 and 0.020 at 30 km/h, 24 km/h and 16 km/h, respectively. The largest MPS was recorded in either the 6th or 7th rib, due to the arm trapped between the side airbag and the thorax. Figure 6 reveals the direction of principal strain with the SBPT at 30 km/h by colored vectors. The red and yellow long arrows indicate that large strain was recorded in ribs 4 through 7 along the longitudinal direction.

The difference of the MPS with and without the SBPT at 30 km/h was difficult to show the difference of their

predicted NFR due to their large MPS compared to the fracture threshold. Whereas, the MPS without the SBPT at 16 km/h was slightly smaller than the fracture threshold thus the increase of the MPS by the SBPT activation influenced on the predicted NFR.

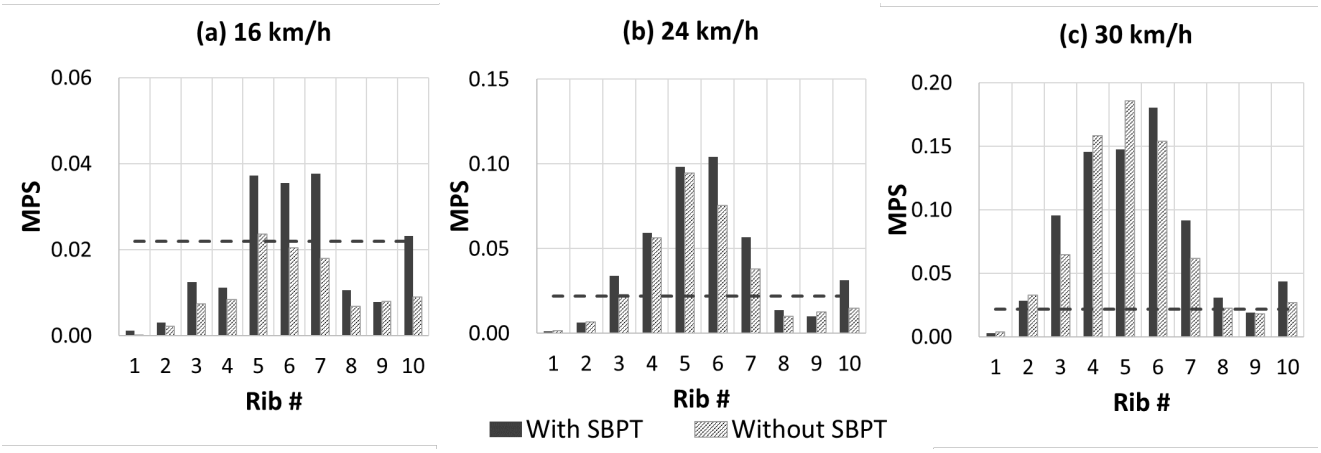

Fig. 5. MPS of each rib in each impact velocity

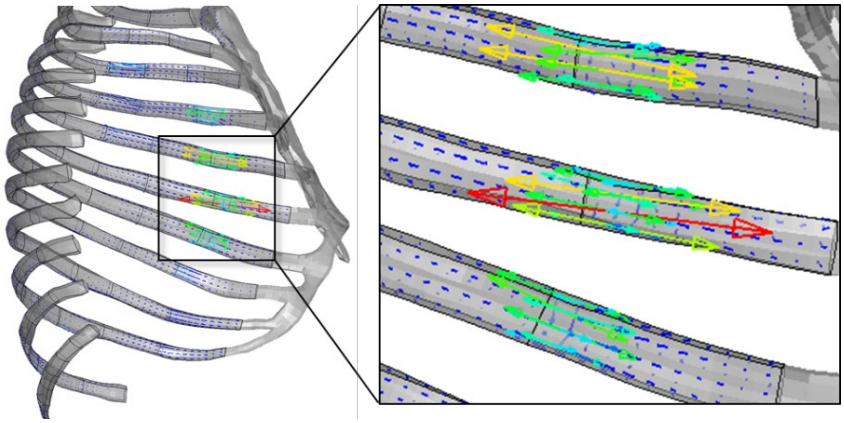

Fig. 6. The direction of principal strains

The results of the maximum lateral and A/P deflection with and without the SBPT are shown in Figure 7 and Figure 8, respectively. The larger the delta-V was, the larger the lateral thoracic deflection was, which was consistent with the relationship between the MPS and delta-V. However, the maximum lateral deflection in an SBPT activation was small compared to that without the SBPT in all three delta-V, whereas the MPS increased by an SBPT activation.

The SBPT activation resulted in maximum A/P deflections ranging between approximately 1 mm and 7 mm at each delta-V. The maximum A/P deflection in each delta-V were 4.9, 3.4 and 6.8 mm at 16, 24 and 30 km/h, respectively.

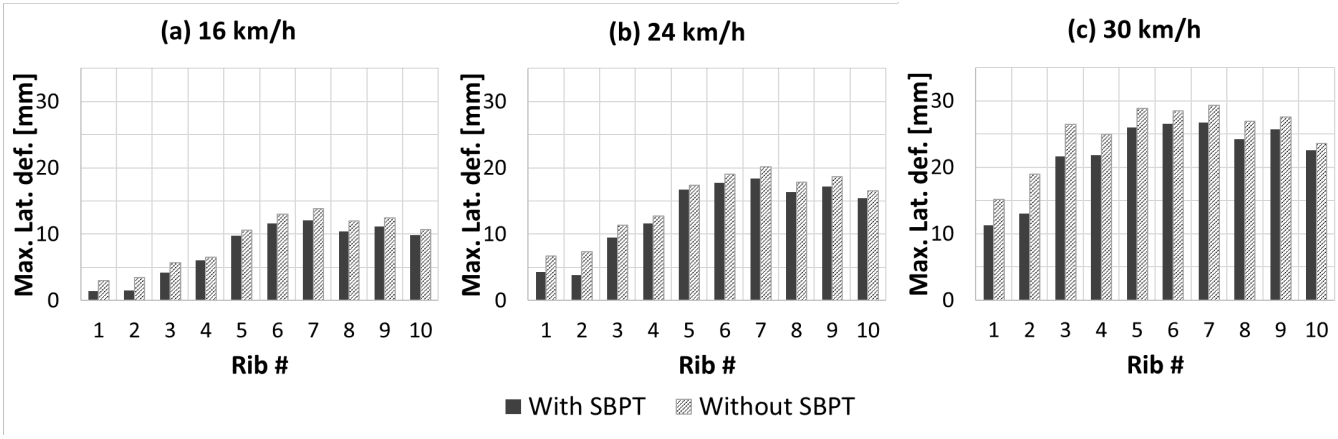

Fig. 7. Maximum lateral deflection at each velocity

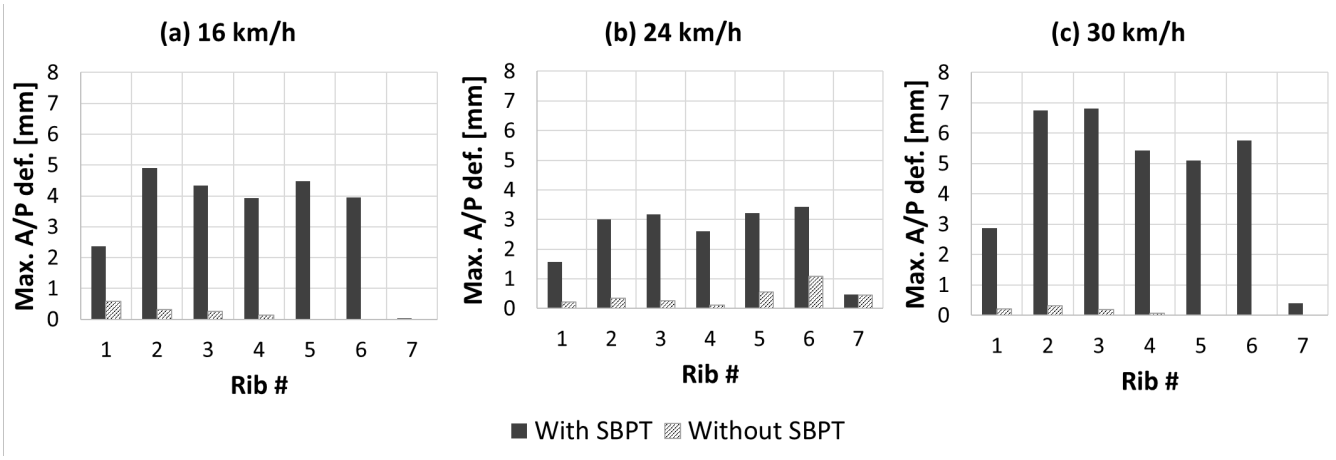

Fig. 8. Maximum A/P deflection at each velocity

The relationship between the predicted NFR and the injury metric

Figure 9 shows the plots of the predicted NFR and three injury metrics calculated from the simulations at each delta-V. As mentioned before, the lateral deflection was reduced by the SBPT activation in spite of an increase of the MPS. This resulted in the reverse relationship between predicted NFR and LCmax in each delta-V, whereas both BRI and TAI took the reverse relationship into account. R^2 were 0.76, 0.87 and 0.88 for LCmax, BRI and TAI, respectively. The combination of the A/P and lateral deflection improved the R^2 from the lateral deflection alone.

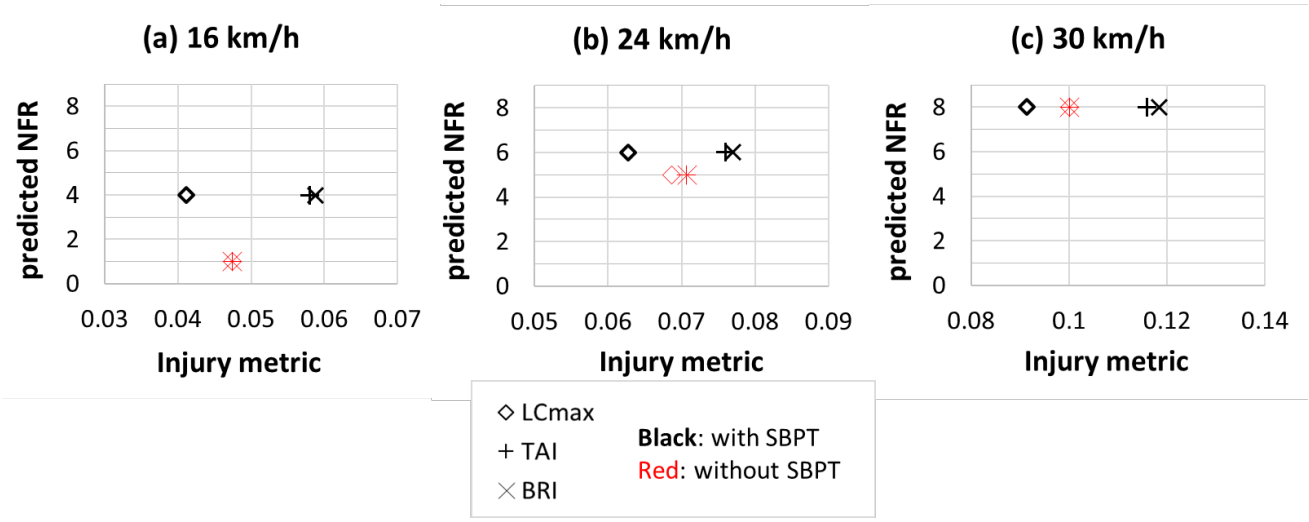

Fig. 9. The plots of the injury metrics and the predicted NFR at each velocity

IV. DISCUSSION

In the accident data analysis, both delta-V groups showed the larger mean NFR with the SBPT than that without the SBPT. However, it should be noted that this analysis included limitations. At first, as the analysis used a convenience sampling, it does not represent real-world injury distributions. Second, the sample size was so small in order to complete information about a specific NFR, a status of an SBPT activation and delta-V to elderly female occupants involved in a near-side crash in NASS-CDS and CIREN databases. Furthermore, the study does not consider the effects of multiple confounding factors on the NFR such as vehicle types and sizes, and the status of other restraint systems such as a side airbag due to shortcomings of the samples. Such small-sized samples including multiple confounding factors generally impair the accuracy of Student t-test.

In this study, rib fracture was represented by the MPS in rib cortical bone which exceeded the fracture threshold determined by the results of coupon tensile tests [19]. It was considered proper to use the tensile test result because the direction of the MPS was along the longitudinal direction of the rib as shown in Figure 6.

HBM simulations conducted in this study revealed that the SBPT increased the predicted NFR at 16 and 24 km/h. Typically this small increase might be deemed acceptable, however, NFR is highly associated with a rise in a fatality rate of the elderly population, which were 12%, 22% and 29% on average for the NFR of 1 and 2, 3 and 4, and 5 and 6, respectively [7][20-21]. The reason why the increase of NFR raises the fatality rate is presumed to be its association with further complications such as pneumonia.

The results of the HBM simulations showed that the SBPT activation increased the predicted NFR, while decreasing the lateral deflections. Therefore, an injury metric based on the pure lateral deflection was concerned to underestimate the predicted NFR in the SBPT activation. In contrast, an increase of the combination of A/P and lateral deflection corresponded to an increase of the predicted NFR, regardless of the SBPT activation.

Regarding the cause of the increase of the MPS by the SBPT activation, it was presumed to be associate with the anterior ribs bent by the combination of the lateral force from the door intrusion and the seat belt constraint force transmitted through the sternum and the costal cartilage. Figure 10 shows that the largest amount of the increase of peak MPS in the SBPT activation was seen in the anterior thorax among three separated regions. These results that pointed to the anterior region corresponded to the results which rib fractures occurred in the similar region in the PMHS sled test [12].

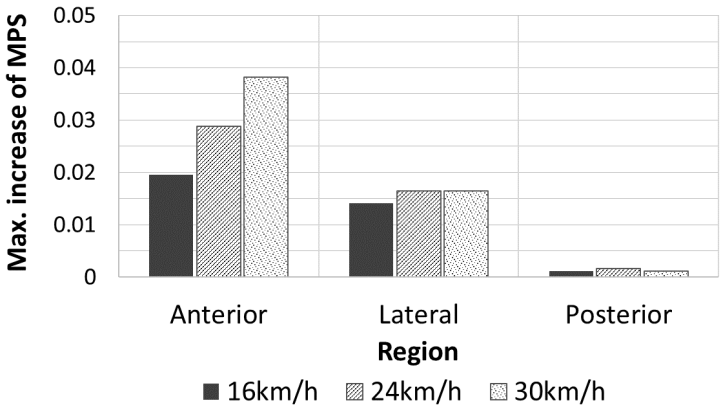

Fig.10. The amount of increase of maximum MPS among 1st to 10th rib in each region by the SBPT activation

Figure 11 shows an overlaid figure of the 6th ribs with and without SBPT at 30 km/h, which are deformed by the combined load from the arm, the side airbag and the seat belt. The coordinate system was fixed at the left costovertebral joint. The left side is the impacted side and a translucent seat belt in the SBPT activation is shown in the figure. The cross-sectional load was measured at the cross-section indicated by A to A' (AA') in the anterior region of the rib. Figure 12 shows that the maximum value of shear-force on the cross-section in the SBPT activation was larger than that in the SBPT activation between 24 and 34 ms. The increase of the shear-force was considered to be due to the seat belt constraint force transmitted through the sternum and the costal cartilage. The increased force caused a deflection on the anterior region of the rib in the struck side, which resulted in increasing the peak strain. Therefore, it was presumed that the peak strain on the anterior region of the rib was

increased by the combination of the A/P and lateral deflection.

The mechanism of the increase in peak strain corresponded to the assumption of BRI, that a steeper curvature of the rib increases the likelihood of fracture. Similarly, TAI using the product of the lateral and A/P compression indirectly correlates with the increase of strain on the anterior rib because the combination of the lateral and A/P compression increases the rib curvature, which generally increases tensile strain on the rib.

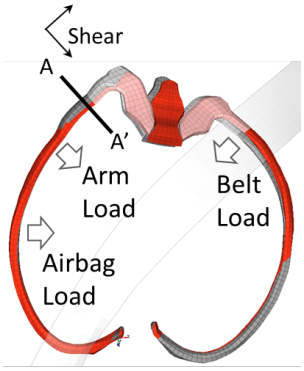

Black: With SBPT
Red: Without SBPT

Fig. 11. Deformation mechanism of the rib in the simulation

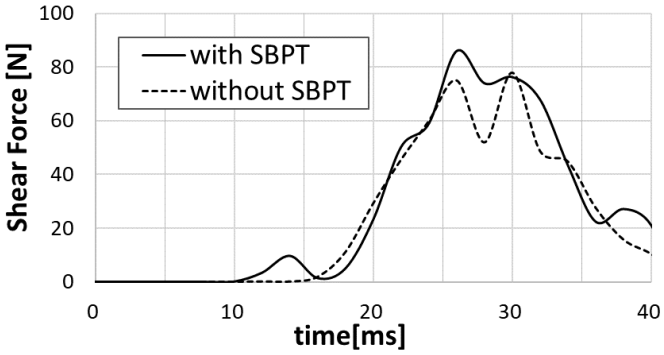

Fig. 12. Shear-force on the cross-section at AA'

Figure 13 illustrates the overall generic trend, showing that the amount of A/P deflection is smaller than that of the lateral deflection, the amount of the lateral deflection increases as the delta-V increases, and the increase in the predicted NFR decreases as the delta-V increases. This may suggest that the contribution of A/P deflection to the increase of the predicted NFR increases as the delta-V decreases. However, the results are presented only to show the generic trend, without showing any quantitative relationships between normalized A/P deflection and the increase of the predicted NFR, due to the lack of sufficient number of simulation runs.

The ratio of A/P deflection and lateral deflection showed a nonlinear relationship with the delta-V. This was because the maximum A/P deflection varied as the delta-V changed, 4.9, 3.4 and 6.8 mm at 16, 24 and 30 km/h, respectively, although the same SBPT configuration was applied. The variation of the A/P deflection may be caused by the difference in the location of the seat belt relative to the thorax. The seat belt path during impact can be influenced by the concurrence of the SBPT activation and the seat belt D-ring intrusion. This complicated mechanism also needs to be further investigated to quantitatively discuss the influence of the A/P deflection.

Regarding MPS on 5th rib without the SBPT at 30 km/h which was large compared to that with the SBPT, it was assumed to be due to the relationship between the rib cage geometry and the arm location.

The lateral deflection without the SBPT tends to be large because no bolster exists on the non-struck side. This would be the reason why the lateral deflection without the SBPT was larger than those with the SBPT.

As other limitation of this study, the individual difference of geometry and material property of both ribs and costal cartilage was not included, which would contribute to the rib deflection in the anterior region. Costal cartilage calcification, which alters the stiffness of the material [22], would influence on the degree of the increase of the strain during rib bending. Additionally, the effect of the SBPT and the injury metrics discussed in this study were verified only by small simulation samples limited to the elderly female occupants. Further verifications are required by increasing the number of samples.

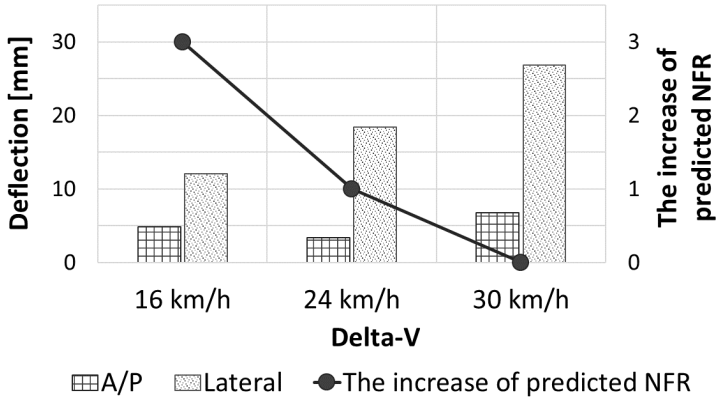

Fig.13. The maximum A/P and Lateral deflections at each delta-V in the SBPT activation

V. CONCLUSIONS

The simulation results by the elderly female HBM showed that the contribution of A/P deflection to the increase of the predicted NFR increases as the delta-V decreases. The study found that the SBPT increased the predicted NFR despite overall lateral deflection decreasing. Therefore, injury risk curves based only on lateral deflection may be underestimating rib fracture probability. Proposed injury metrics that include A/P deflection, which were BRI and TAI, showed better correlation with strain than those based on pure lateral deflection.

VI. REFERENCES

[1] NHTSA-National Highway Traffic Safety Administration, (2020) Traffic Safety Facts 2018, DOT HS 812 981.
[2] NHTSA-National Highway Traffic Safety Administration, (2005) Characteristics of Crash Injuries among Young, Middle-Aged, and Older Drivers, DOT HS 810 857.
[3] Ortman, J. M., Velkoff, V. A. Hogan, H., (2014) An Aging Nation: The Older Population in the United States, United States Census Bureau
[4] Ramachandra, R., Kashikar, T. Bolte IV, J., (2017) Injury Patterns of Elderly Occupants Involved in Side Crashes, The proceedings of International Research Council on Biomechanics of Injury (IRCOBI) Conference, 2017, Antwerp, Belgium.
[5] NHTSA-National Highway Traffic Safety Administration “NHTSA Crash Viewer, NASS CDS (2004-2015) Search” , https://crashviewer.nhtsa.dot.gov/LegacyCDS/Search, [Accessed 28 August 2020]
[6] NHTSA-National Highway Traffic Safety Administration “NHTSA Crash Viewer, CIREN (2004-2015) Search”, https://crashviewer.nhtsa.dot.gov/LegacyCIREN/Search, [Accessed 28 August 2020]
[7] Stawicki, S. P., Grossman M. D., et al., (2004) Rib Fractures in the Elderly: A Marker of Injury Severity, Journal of the American Geriatrics Society. 52(5): p.805-808.
[8] Stalnaker, R. Mohan, D., (1974) Human Chest Impact Protection Criteria, SAE Technical Paper 740589
[9] Tarriere, C., Walfisch, G., et al., (1979) Synthesis of human tolerances obtained from lateral impact simulations, The Proceedings of the 7th International Technical Conference on Experimental Safety Vehicles (ESV), 1979, Paris, France
[10] Cavanaugh, J., Zhu, Y., Huang, Y. King, A., (1993) Injury and Response of the Thorax in Side Impact Cadaveric Tests, SAE Technical Paper 933127
[11] Kuppa, S., Eppinger, R., et al., (2000) Assessment of Thoracic Injury Criteria for Side Impact, Proceedings of International Research Council on Biomechanics of Injury (IRCOBI) Conference,2000, Montpellier, France
[12] Eppinger, R., Marcus, J. Morgan, R., (1984) Development of Dummy and Injury Index for NHTSA's Thoracic Side Impact Protection Research Program, SAE Technical Paper 840885
[13] ISO/TC 22/SC 36, (2013), ISO/TR 12350:2013 Road Vehicles – Injury Risk Curves For the Evaluation of Occupant Protection in Side Impact tests
[14] Shurtz, B. K., Agnew, A. M., Kang, Y.-S. Bolte IV, J., (2018) Application of Scaled Deflection Injury Criteria to Two Small, Fragile Females in Side Impact Motor Vehicle Crashes, SAE Technical Paper 2018-01-0542
[15] Sugaya, H., Takahashi, Y., et al., (2019) Identification of Accident Representative Scenario for Elderly Female

Occupants in Side Impact, International Journal of Automotive Engineering, 10(2): p.150-155.
[16] Dokko, Y., Yanaoka, T. Ohashi, K., (2013) Validation of Age-Specific Human FE Models for Lateral Impact, SAE Technical Paper 2013-01-1242
[17] Robbins, D. H., (1983), Anthropometric Specifications For Small Female And Large Male Dummy, Volume3. FINAL REPORT, Oct: UMTRI-83-53-3
[18] Sugaya, H., Takahashi, Y., et al., (2019) Development of a Human FE model for Elderly Female Occupants In side Crashes, The Proceedings of 26th International Technical Conference on Enhanced Safety of Vehicles (ESV), 2019, Einthoven, Netherland
[19] Kemper, R. A., McNally C., et al., (2005) Material properties of human rib cortical bone from dynamic tension coupon testing, Stapp Car Crash Journal 49: p.199-230
[20] Bergeron, E., Lavoie, A., et al., (2003). Elderly trauma patients with rib fractures are at greater risk of death and pneumonia, The Journal of Trauma: Injury, Infection, and Critical Care, 54(3): p.478-485
[21] Bulger, E. M., Arneson, M. A., Mock, C. N. Jurkovich, G. J., (2000) Rib Fractures in the Elderly, The Journal of Trauma: Injury, Infection, and Critical Care, 48(6): p. 1040-1047
[22] Holcombe, S., Ejima, S. Wang, S., (2017) Calcification of Costal Cartilage in the Adult Rib Cage, The Proceedings of International Research Council on Biomechanics of Injury (IRCOBI) conference, 2017, Antwerp, Belgium